Selective laser photodetachment of intense atomic and molecular negative ion beams with the ILIAS RFQ ion beam cooler

Martin Martschini[1‡], Johanna Pitters[1,2], Tobias Moreau[1], Pontus Andersson[1,3], Oliver Forstner[1,4], Dag Hanstorp[5], Johannes Lachner[1], Yuan Liu[6], Alfred Priller[1] Peter Steier[1], Robin Golser[1]

[1] University of Vienna, Faculty of Physics – Isotope Research, VERA Laboratory, Währinger Straße 17, A-1090 Vienna, Austria

[2]CERN, Geneva 23, 1211 Switzerland

[3]FluxSense AB, SE-412 96 Gothenburg, Sweden

[4]Friedrich-Schiller-Universität, 07743 Jena, Germany

[5]Department of Physics, University of Gothenburg, SE-412 96 Gothenburg, Sweden

[6]ORNL Oak Ridge National Laboratory, Tennessee, USA

[‡]Corresponding author: martin.martschini@univie.ac.at

Keywords: AMS; ion beam cooling; selective laser photodetachment; optical filtering; negative ions

Abstract

The Ion Laser InterAction Setup (ILIAS) project at the University of Vienna aims at the exploration of negative ion beam filtering by selective laser photodetachment for applications in accelerator mass spectrometry (AMS). A gas-filled radio frequency quadrupole (RFQ) is used to decelerate and cool negative atomic and molecular ion beams with intensities of up to several hundred nA, and overlap them collinearly with a continuous wave (cw) laser beam. Ion-laser interaction times ranging from 500 μs to several ms allow for highly efficient, selective photodetachment depletion of disturbing ion species within these beams. The elemental selectivity of this technique is based on the differences in electron affinities, and therefore does not depend on relative differences in atomic numbers. It may therefore provide sufficient isobar suppression for new trace isotopes, which are not accessible with existing AMS techniques.

The ILIAS RFQ cooler was characterized at a purpose-built test bench with respect to ion beam transmission, ion cooling capabilities and ion residence times as a function of injected ion current to assess its suitability for future AMS use. A $^{63}Cu^-$ test beam of 600 nA was

photodetached with more than 99.999% efficiency with a 532 nm laser at 10.8 W power. At the same time, ions of interest having electron affinities higher than the photon energy passed the cooler unaffected. Total ion losses were thus found to be below 50% of the sputter source output. Finally, first photodetachment experiments in connection with ^{26}Al detection demonstrated selective isobar suppression of MgO^- vs. AlO^- by more than 4 orders of magnitude.

Currently, the RFQ cooler is moved to a new injector beamline at the Vienna Environmental Research Accelerator (VERA) for first applications of this novel technique at a state-of-the-art AMS facility.

1. Introduction

The study of trace isotopes with typical isotopic abundances of 10^{-10} down to 10^{-16} has become an essential tool in various fields of research including archaeology, geology, oceanography, astrophysics and many other environmental research disciplines [1]. Accelerator mass spectrometry (AMS) [1, 2] often is the measurement technique of choice providing by far the highest abundance sensitivities. In many cases however, atomic isobaric interferences constitute a major limitation for the study of trace isotopes by AMS [2]. Element-selective filtering of negative ion beams is an emerging technique with potential to overcome this problem [3, 4]. These new techniques are expected to provide significant improvement, especially in the mass range of 60 amu and above where relative differences in atomic number $\Delta Z/Z$ between isobars become too small to be exploited at AMS facilities with terminal voltages ≤ 10 MV. Until recently, existing isobar separation techniques were all based either on the difference in energy loss characteristics or the difference in mean charge state of the elements when passing through matter (see e.g. [5] for a review of existing techniques). As these methods generally require ion energies of several MeV or more, they can only be employed at the high energy side of AMS facilities, typically directly in front of or as part of the detection system. Unfortunately, the isobar separation power of these techniques decreases with increasing nuclear charge and strongly depends on the attainable beam energy.

In contrast, the new element-selective filtering techniques exploit the differences in electronic structure of the ions of neighboring elements. They require slow negative ion beams and are hence employed at the low energy side of AMS systems. Most importantly, they provide similar isobar separation powers for heavy nuclides as for light ones, independent of the terminal voltage. Thereby, new trace isotopes like ^{93}Zr, ^{135}Cs or ^{182}Hf may for the first time become

accessible with AMS at their environmental abundances [6, 7, 8]. Additionally, trace isotopes like ^{60}Fe or ^{53}Mn, for which measurements can only be conducted at a few large AMS accelerators worldwide, will become accessible at smaller, more cost-effective and efficient AMS machines.

To our knowledge, there are two approaches for element-selective filtering of anion beams under close investigation: chemical anion-gas reactions including resonant charge transfer in a gas reaction cell [9, 10] and optical filtering by laser photodetachment [11, 12, 13]. Both methods require slowing down the negative ions from several ten keV – the energy typically provided by sputter ion sources – to eV or sub-eV energies. In the case of laser photodetachment, this deceleration substantially increases the interaction time of the ion beam with the laser to attain the necessary detachment efficiencies for the unwanted ion species. The reaction cell method on the other hand requires ion beam energies below a few eV to avoid unintended neutralization of the fragile anions of interest in collisions with the reactive gas.

The main prerequisite for the applicability of optical filtering by photodetachment is that the ion of interest has a higher electron affinity (EA) than the interfering isobar. Generally, the EA is defined as the energy difference between the ground states of an atomic or molecular negative ion and its corresponding neutral, although the situation for molecular anions is much more complex due to vibrational and rotational states as well as possible changes in nuclear configuration between the anion and its neutral [14]. In case the atomic anions of the isobar system under investigation have unsuitable EAs for laser photodetachment, one has to find a proper molecular system. A list of possible ion systems for several trace isotopes of interest is given in [13].

Laser photodetachment is the process of removing the weakly bound extra electron from an anion by means of laser radiation

$$R^- + h\nu \rightarrow R + e^-, \qquad (1)$$

where R respresent an atom or molecule, h Planck's constant and ν the frequency of the incoming photon. It is a threshold process and can occur as soon as the photon's energy is equal or larger than the EA of the atom, assuming the anion is in its ground state. If it is in an excited state, the threshold for photodetachment is shifted towards lower photon energies. For a more thorough description see [14, 15]. When interacting with laser light, the number of ions from an ion species with EA smaller than the photon energy decreases with interaction time t according to

$$N(t)=N(0)\cdot e^{-\sigma\Phi t}$$

with σ being the cross section and Φ the photon flux. Cross sections for laser photodetachment are rather small, typically several 10^{-17} cm^2. Commercially available cw lasers provide output powers of several Watts corresponding to a photon flux between 10^{20} and 10^{21} $cm^{-2}s^{-1}$ assuming reasonable focusing. Since interfering isobars have to be reduced by several orders of magnitude for AMS applications, the laser ion interaction time has to be at least on the order of several hundred μs. This can only be achieved by substantial deceleration of the keV ions in an ion beam cooler as ion laser overlaps of several hundreds of meters are not feasible.

An advantage of the laser photodetachment approach is that there is no need to maintain a defined ion energy over the whole length of the cooler for efficient filtering opposed to e.g. reaction cell separation of CaF_3^- and KF_3^- [9]. As long as the maximum storable charge of the cooler is not approached, a completely thermalized ion beam and thus a longer residence time inside the ion cooler is even advantageous, which simplifies the setup significantly.

At the Vienna Environmental Research Accelerator VERA, the development of a dedicated ion cooler for negative ions was initiated in 2010. For this purpose, the ILIAS (Ion Laser InterAction Setup) test bench was constructed. It consists of a negative-ion mass spectrometer providing mass-separated ion beams of up to 300 u with a maximum energy of 30 keV from a single-cathode cesium sputter ion source. The detailed layout of ILIAS was recently described in [13]. In the following, the ion beam cooler and its performance are discussed and first photodetachment experiments with intense negative ion beams of up to a few μA are presented.

2. The ILIAS RFQ ion beam cooler

The ILIAS RFQ ion beam cooler is a non-segmented linear Paul trap filled with buffer gas to dampen the ion motion. In the radial direction, the ions are confined by the RF quadrupole field whereas a weak electric field guides the ions along the beam axis towards the exit. Buffer gas cooling of ion beams inside RFQ ion guides is a widely used technique [16 - 19], however with the exception of [17] all of these coolers were constructed to be used with positive ions. The fragility of negative ions sets a few constraints on the design of the ion cooler. Most importantly, the center-of-mass energy in collisions with gas atoms must not exceed the EA of the ions of interest in order to avoid unwanted collisional neutralization. In practice, this means that the keV ion beam has to be electrostatically decelerated to a few tens of eVs before injection into the buffer gas and that the buffer gas has to be as light as possible to minimize the energy transfer per collision. Hence, He is used as buffer gas.

At ILIAS, the whole cooler assembly including the required electronics is mounted on a high-voltage platform, which can be set to a potential between 0 kV and –30 kV to electrostatically decelerate the ions. A system of aperture lenses on either side of the cooler ensures smooth field gradients and proper focusing of the ion beam into and out of the cooler tube apertures. On the injection side, this system has to compensate for the increase in angular divergence of the beam during deceleration. Additionally, these aperture lenses act as pumping barriers to minimize leakage of buffer gas into adjacent beamline sections. The design of the lens system is based on simulations with SIMION 8.0 (Scientific Instrument Services, Inc., Ringoes, NJ, USA) [20]. A schematic of the cooler assembly is shown in Figure 1(a). The cooler electrode structure is placed inside a cylindrical tube with 40 mm inner diameter. Insulated metal apertures with 3 mm diameter terminate the cooler tube at both ends such that any ion current on them can be measured via a BNC feedthrough. These cooler tube apertures also define the size of the ion laser interaction region as the 3 mm laser beam passes through them. The buffer gas inlet is in the middle of the cooler tube and the buffer gas flow is adjusted via a manually controlled leakage valve outside the vacuum chamber. The buffer gas pressure is monitored with a Pirani ion gauge directly connected to the gas inlet tube. Typical pressures for ion cooling with He are around 0.2 mbar. The buffer gas exits the cooler tube at both ends through large pumping holes in the tube wall as well as the aperture openings. Movable sleeves allow adjustment of the size of the pumping holes at both ends. During experiments however it turned out that both the beam transmission through the cooler as well as the gas flow to adjacent beamline sections depends only on the pressure in the center of the tube and is independent of the size of the pumping holes. Therefore, the pressure profile along the cooler tube seems to be mainly determined by the flow resistance of the cooler tube's interior rather than by the size of the pumping holes at either end. Turbo molecular pumps with pumping powers for He of 1270 l/s and 650 l/s, respectively, efficiently remove the buffer gas from the beamline volume around the cooler tube in a differential pumping system, where the aperture lenses act as pumping barriers towards adjacent beamline sections. Experimental pressure values are given in Figure 1(a).

The electrode structure of the ILIAS cooler has a length of 951 mm and consists of four cylindrical rods to produce the RF field and four DC-guiding electrodes to create a weak electric field along the beam axis. The guiding electrodes are 1.5 mm thick plates with rounded edges at a negative potential with respect to the RF rods and the cooler tube. They are placed between the RF rods and are slightly tilted with respect to the longitudinal cooler axis such that the inscribed radius increases from entrance to exit by 0.6 mm over the entire length of 951 mm. The quadrupole rods have a radius of $r = 5.00$ mm and an inscribed radius of $r_0 = 4.35$ mm, with

the ratio r/r_0 being close to the theoretically best value of 1.1468 for a pure quadrupole field with cylindrical electrodes inside a round tube [21]. The electrode structure is held in place by 6 ceramic spacers made of Macor, which are equally distributed over the whole length of the cooler. Photos of the electrode assembly and the cooler tube are shown in Figures 1(b) and 1(c). When no additional DC-voltage is applied to the RF-rods, the ion cooler acts as a high-pass mass filter ion guide. Ion motion inside the cooler is governed by the Mathieu-parameter $q = \frac{4QV_{RF}}{mr_0^2\Omega^2}$ with Q and m being the charge and mass of the ion, V_{RF} the RF zero-to-peak voltage, Ω the angular RF frequency and r_0 the inscribed radius of the RF-electrodes. Stable trajectories inside the cooler exist for all masses with q<=0.908. A detailed discussion of ion motion inside a linear Paul trap can be found in e.g. [22]. Highest transverse confinement is achieved at q=0.5-0.6, at higher values of q the RF-driven micromotion leads to larger amplitudes in the radial motion of the ions [18] (cf. Figure 3(a) for experimental data with the ILIAS cooler). For values of q below 0.5, the confinement of ions in radial direction can be approximated by a pseudo-potential well with depth $D = \frac{qV_{RF}}{4}$ [22]. Since D determines the maximum storable charge of cooled ions and thus the maximum current that can be transmitted through the cooler without beam losses due to space-charge effects, the design goal was to achieve zero-to-peak RF voltages of 400 V for all ions.

The RF setup for all experiments described in the following consists of a function generator (Stanford Research Systems DS345), which provides a sine wave signal with an amplitude of typically 0.1 V, and a subsequent 400 W RF power amplifier (Electronics & Innovation, Ltd. model 1040 L), which feeds the primary circuit of a ferrite transformer. On the secondary side, two non-resonant circuits are coiled in inverse direction with a 180° phase shift, each one driving two opposite rods of the quadrupole. This setup allows zero-to-peak voltages of 200 V and a maximum frequency of 2 MHz, limited by the high reflected power and the maximum power transmission of the ferrite transformer. For future studies, a resonant setup has recently been commissioned to overcome these limitations. In this new setup, the two resonant circuits on the secondary side of the ferrite transformer can be tuned at the desired frequency by a 9 binary digit set of inductors to match the capacitance of the cooler of around 300 pF. This setup provides zero-to-peak voltages of 400 V in the frequency range of 1.2 - 6 MHz and typically requires only around 50 W RF power from a 200 W amplifier (Electronics & Innovation, Ltd. model 1020 L). Hence, it will allow optimal cooling of ions with masses between 14 u and 350 u at the full 400 V zero-to-peak voltage. For ions outside this mass range, the RF-voltage has to be adjusted accordingly, i.e. 340 V at 6 MHz for ^{12}C.

3. Experimental results and discussion

3.1 Performance of the RFQ ion beam cooler

Cooling of ion beams

The main purpose of the ILIAS cooler is to extend the interaction time of anions with the laser light. The reduction of beam phase space at the same time is a welcome feature but not a prerequisite as any subsequent AMS system is usually designed to accept the full phase space emitted from the ion source. Once the anions enter the buffer gas region, their momenta after electrostatic deceleration are gradually reduced by interactions with the light buffer gas. Thereby, they are not only slowed down but the amplitudes of their oscillations in transverse direction become smaller and they migrate towards the center of the cooler. Subsequently they stay longer within the 3 mm diameter region of the laser, which further increases the laser anion interaction time. The reduction in beam size can also be observed experimentally by monitoring the transmitted ion current and the current on the exit aperture of the ion cooler as a function of buffer gas pressure. Data from an experiment with AlO^- is shown in Figure 2. Without any buffer gas, almost half of the ions that enter the cooler tube through the 3 mm entrance aperture have a distance of more than 1.5 mm from the cooler axis at its exit and thus hit the 3 mm exit aperture contributing to the measured aperture current. Furthermore, several ions also have trajectories with too large transverse oscillation amplitudes and thus leave the potential well of the central cooler area causing further beam losses. With increasing buffer gas pressure, the transmitted current increases as the beam size is reduced and the number of ions hitting the exit aperture becomes negligibly small. The reduction in beam size is of course limited by the repulsion due to space charge and we observe adverse effects when attempting to cool ion beams of 2 μA or above. The slight decrease in transmitted current for very high buffer gas pressures can be explained by increased collisional losses, i.e. ions that are scattered out of the potential well. Additionally, the probability for collisional detachment at injection and extraction increases due to a higher buffer gas flow into these regions.

The cooling process of individual ions within the RF region has been simulated using SIMION with a hard sphere collision model for the buffer gas [20]. These simulations have shown that the anions do not fully thermalize with the gas but retain an average kinetic energy of around 0.1 eV at typical He pressures (0.1 mbar) due to the driving force of the RF field.

Transmission

The transmission of the ion beam through the cooler is a crucial parameter for its suitability for AMS systems. In [13] transmission values of 8% for ion beams of several hundred nA were reported. The transmission is determined as the ratio of measured ion currents in Faraday cups before and after the ion cooler (cf. Figure 5). Installation of xy-steerer plates in front of the injection lens assembly and behind the extraction electrodes brought a substantial improvement in transmission (see [23] for further design details). For currents of a few nA, more than 60% of the ion beam can be injected into the ion cooler, successfully cooled and extracted, which compares well to similar setups elsewhere [24]. All transmission values reported here are measured with the full phase space emitted from the sputter ion source without any ion beam collimation apertures prior to the injection current measurement. Figure 3(a) shows the dependence of the transmission for various ions on the RF settings of the ILIAS cooler. Optimum transmission is achieved with the Mathieu parameter q between 0.4 and 0.5. Experimental transmission values with a 23 keV $^{63}Cu^-$ test beam as a function of injected ion current are plotted in Figure 3(b). The obvious decrease in transmission at currents above 100 nA can be attributed to space charge effects, both in the ion source and inside the cooler. A higher emittance of the ion beam from the source reduces the injection efficiency into the ion cooler, which can be monitored via the current on the injection aperture. Additionally, the accumulated charge inside the ion cooler leads to increased particle repulsion which blows up the cooled ion beam. The latter effect also motivates improvements on the RF setup, as described in section 2, since the maximum storable charge inside the cooler is expected to increase for higher RF-amplitudes [25].

A crucial issue regarding anion beam transmission is electron detachment in collisions with He buffer gas. $^{63}Cu^-$ has an EA of 1.23578(4) eV [15], thus one may intuitively expect collisional detachment to occur above this collision energy in the CM frame, i.e. 20.7 eV in the lab frame. However, for several anions like O^- and F^-, experimentally observed threshold energies for electron detachment in collisions with He are significantly higher than their EAs [26, 27]. We attribute this to the low probability for head-on collisions with complete energy transfer. In addition, the optimum injection energy is always a tradeoff between collisional detachment and beam losses due to increased angular divergence of the beam as a result of the deceleration.

During the experiments it turned out that the highest beam transmission with $^{63}Cu^-$ is achieved at injection energies around 50 eV. Also for several other ions in this study like e.g. AlO^-, the optimum injection energy into the buffer gas was found to be such that the collision energy in the CM frame equals roughly twice the EA. Unfortunately, there does not seem to exist a general rule to that problem and no experimental data on collisional detachment thresholds for

these ions are known to the authors. A good overview is given in the review by Champion [28]. Therein, also collisional detachment thresholds well below the EA are reported for certain molecular anions like O_2^- and linked to populated excited vibrational states [29]. We do observe a similar behavior for MgO^- (cf. Figure 8), although other mechanisms of ion loss cannot be excluded at this stage.

Residence time

The laser induced isobaric suppression factor can be calculated if the photon flux, the photodetachment cross sections and the residence time of the ions inside the cooler is known. During modelling of the cooler, the ion residence time inside the RFQ was simulated with SIMION[1] and a hard sphere collision model as well as a damping model for the buffer gas [20]. These simulations yield residence times around 10 ms for individual ions at a uniform buffer gas pressure of 0.1 mbar He. However, the actual residence times may differ a lot from this value as the actual gas density distribution inside the RFQ is unknown and space charge effects, that will additionally push ions towards the exit, were not included.

The residence time of ions inside the ILIAS cooler was finally measured via time-of-flight measurements with a $^{63}Cu^-$ test beam [Ref Moreau]. Electrostatic steerer plates in front of the mass analyzing magnet were used to deflect the ion beam into or away from the RFQ cooler (cf. Figure 5 for a schematic view of the setup). A fast high voltage transistor switch (HTS 51 from Behlke Power Electronics, Kronberg im Taunus, Germany) allowed applying voltage to one of the steerer plates with a rise time from zero to full voltage of 0.5 µs. The time constant when grounding the plate again was around 70 ms. Hence, the system could be tuned such that either the rising or the falling edge of the chopped ion beam had a sharp time characteristic. A rectangular voltage signal from a function generator was used to actuate the Behlke voltage transistor switch.

The ion current transmitted through the RFQ was measured with a SRS SR570 current amplifier (Stanford Research Systems, Sunnyvale, California, USA) connected either to a Faraday cup or the anode of a micro-channel plate detector. The MCP detector was used to detect transmitted currents of a few nA and below. At these low currents, a direct recording of the ion current time structure with the Faraday cup is hindered by the low-pass behavior of the SRS amplifier in the

[1] Only the latest code version SIMION 8.1 (Scientific Instrument Services, Inc., Ringoes, NJ, US) with surface enhancement by fractional grid units [30] allows to reproduce the longitudinal guiding field of the tilted electrodes with sufficient accuracy.

respective sensitivity ranges. Instead, the MCP (Burle, MCP 25/12/12 D 60:1 TC, PN30298, in a Chevron configuration) was used to amplify the ion signal to several hundred nA. For this purpose, the MCP was operated at 600-700 V, roughly 60-70% of the voltage typically applied for single ion detection. The detector voltage was adapted to the transmitted ion current in order to have an anode current of roughly 200 nA. The equivalency of the two detection methods was tested at 150 nA transmitted ion current by comparison of the Faraday cup signal and the signal from the MCP, which was placed closely behind a 100-fold ion beam attenuator made of a perforated steel plate. The two detection methods yield the same results. The time structure of the SRS amplifier signal was finally recorded with a Tektronix TDS 1002B oscilloscope (Tektronix, Inc., Beaverton, Oregon, USA) triggered to the onset of the steerer plate voltage.

During the experiments buffer gas pressure, guiding field strength, beam chopping frequency and ion beam intensity were varied. The injected ion beam current could be reduced by factors of 100 and 10’000, respectively, via the insertion of one or two 100-fold ion beam attenuators (perforated steel plates) in front of the ion beam cooler. The ion current curves were recorded and averaged over at least 16 beam switching cycles under identical conditions. Assuming the ion beam is bent into the cooler by the steerer (“rising edge”), the ion current curve recorded downstream from the cooler will rise from zero to a plateau with the ion residence time information being contained as the delay and rise time of the rising current edge. Hence, the recorded current curves were differentiated to obtain the ion residence time distributions. The experimental ion residence time distributions from this study are shown in Figure 4. The plotted time is the actual time-of-flight of ions from the electrostatic steerer to the respective detector, which apart from the residence time inside the ion cooler also includes around 40 μs time of flight outside the ion cooler. While both injected ion current and buffer gas pressure strongly shift the maximum of the ion residence time distribution, the strength of the longitudinal guiding field has very little impact even for currents of nA and below. A stronger guiding field only narrows the distribution a bit by reducing the likelihood of very long residence times (cf. Figure 4(a)). This already suggests that the accumulated charge inside the RFQ rather than the guiding field is dominating the ion movement in longitudinal direction.

Subsequently, using either the rising or the falling edge of the chopped ion beam and analyzing the corresponding build-up or drop of ion current intensity after the cooler yields different results for the ion residence time. In the case of the rising edge, i.e. injecting the beam in the empty cooler, a sharp onset of the ion current is followed by an initial build-up of charge inside the RFQ, thus first ions tend to reside longer than under continuum conditions. A sharp drop in ion current on the other hand reflects continuum conditions in the beginning and only the last

ions experience significantly less space charge effects. This causes a slightly more pronounced tail towards long residence times than under continuum conditions. Additionally, a beam chopping frequency dependent time lag was observed when studying the rising edge of the ion beam pulses. When the length of the individual ion current pulses was kept constant, a higher number of current pulses per second resulted in smaller residence times, more similar to the distributions obtained from the falling edge. The reason behind this behavior is not understood yet and requires further investigations. Since the time between individual beam pulses was still much longer than the measured ion residence times, it seems unlikely that this effect is caused by residual ions inside the RFQ. The fact that the magnitude of the effect decreased with higher currents, could possibly be explained by some charging of surfaces inside the ion cooler. To avoid this problem, the falling edge, which did not show any of such effects, was chosen for the experiments presented below.

Without buffer gas, the mean ion residence time is 0.12 ms with an FWHM of 0.15 ms at an injection energy of 50 eV. This time is almost independent of the injected current as space charge effects are rather small for the uncooled ion beam. With increasing buffer gas pressure, the ion residence time distribution is, as expected, shifted towards longer residence times and significantly broadened (cf. Figure 4(b)). The strength of this effect however not only depends on the buffer gas pressure but also strongly changes with the injected current, as shown in Figure 4(c). For an injected ion current of 3.2 nA, the most probable ion residence time at a pressure of 0.30 mbar is 2.0 ms with an FWHM of the distribution of 3.9 ms and a very pronounced tail towards long residence times (median residence time 3.7 ms). When injecting 340 nA at the same buffer gas pressure, the most probable ion residence time is only 0.5 ms with an FWHM of 0.8 ms and a median of 1.5 ms. Average ion residence times on the order of 10 ms are only achieved when injecting ion currents of several pA or less. At 32 pA, the most probable ion residence time is 8.2 ms with an FWHM of 18.5 ms and a median of 23 ms. Hence, in the limit of low ion beam intensities, where space charge becomes negligible, the SIMION calculations are in reasonable agreement with the measurements. These effects need to be considered when establishing a measurement scheme once the ILIAS-cooler is integrated into an AMS system.

3.2 Laser photodetachment experiments

Laser photodetachment of ^{63}Cu

First experiments with the ILIAS cooler on the depletion of negative ion beams by laser photodetachment were conducted with a $^{63}Cu^-$ beam from a solid copper sputter target. Apart from its suitable EA of 1.23578(4) eV [15], this test ion was chosen because negative ion beams of several μA can readily be extracted from the sputter ion source and exhibit very little molecular impurities at mass 63. This is of importance as there is no suitable means of ion identification available at ILIAS to analyze the composition of the ion beam extracted from the ion cooler. Beam impurities with an EA higher than the photon energy of the laser, which cannot be detached, will add to the transmitted current and therefore mimic lower depletion efficiency for the ion under investigation.

The measurement setup is shown in Figure 5. A more detailed description of the whole ILIAS setup is given in [13]. The mass-separated ion beam is injected into the RFQ ion cooler and overlapped with the laser beam, which goes anticollinearly through the RFQ. After the RFQ-cooler, the transmitted ion beam is bent out of the laser beam by means of an electrostatic quadrupole beam bender and subsequently is measured in a Faraday cup. The laser system for these experiments was a VERDI V18 (Coherent Inc., Santa Clara, CA, USA) providing 18 W of continuous wave 532 nm (2.33 eV) laser light. The beam has a Gaussian-shaped power profile with a $1/e^2$ width of 2.2 mm at the 3 mm ion cooler extraction aperture. The maximum power inside the ion cooler is around 13.5 W. The transmitted power is measured with a calorimetric power head S310C (Thorlabs Inc, Newton, NJ, USA) at the straight port of the bending magnet. The power at this point is 15% lower than the actual laser power inside the ion cooler owing to 10% transmission loss at the borosilicate viewing port in front of the power head and 5% power loss at the 3 mm cooler aperture, through which the laser exits. The laser power can be adjusted without influencing the shape of the power profile by external rotation of the light polarization plane and subsequent beam splitting with a polarizing beam splitter.

In order to determine the suppression by photodetachment, the transmitted ion current was recorded while the laser was turned on and off periodically in intervals of typically 15 seconds each. Figure 6(a) shows experimental data from these experiments. When the laser is off, more than 300 nA of $^{63}Cu^-$ are transmitted through the ion cooler at a He buffer gas pressure of 0.25 mbar. When the laser is turned on, the current immediately drops to around 3 pA at a transmitted laser power of 10.8 W. This is equivalent to a depletion efficiency of 99.999% or a suppression factor of 10^5 respectively. The time constant of the current drop was measured to be below 30 ms, which is the time resolution limit of the data acquisition system. To exclude any general influence of the laser beam on ions independent of their EA, the same experiment was repeated with a $^{127}I^-$ beam (EA = 3.059038(10) eV [15]). The results are shown in

Figure 6(b). The transmitted ion current of 600 nA stays constant no matter whether the laser is on or off. This demonstrates that ions with EAs higher than the photon energy of the laser beam can pass the RFQ cooler unaffected.

Figure 7 shows the suppression of $^{63}Cu^-$ as a function of laser power for three different buffer gas pressures. As expected, a higher buffer gas pressure results in higher suppression values due to longer ion residence times within the laser beam. However, the suppression factor at any buffer gas pressure does not follow a simple exponential increase with the laser power, i.e. the number of photons. Instead, one observes a very steep increase of the suppression factor between 1 – 2 W of laser power, which then flattens out to a moderate increase for laser powers above 5 W. This two-slope behavior has also been observed elsewhere and was attributed to two possible causes: The Gaussian power profile of the laser with complete detachment in the center occurring at lower power than at the wings and 'hot' ions with significantly lower residence times [12]. In addition to the above, also the dependence of the ion residence time on the stored charge inside the RFQ will contribute to this behavior at injected currents of several hundred nA used for this experiment. Once an anion is photodetached, the charge carrying electron is immediately removed from the central RFQ area as there is no stable trajectory for such light particles within the given RF field. Hence, the charge inside the cooler is significantly reduced once a macroscopic fraction of the anions is detached. Subsequently, the remaining anions experience a smaller space charge driven force towards the exit and reside longer within the laser beam. This strong enhancement diminishes as soon as the effect of space charge on the ion residence time becomes small, which is expected for pA currents. This however only applies to ion beams where most ion species of the injected mass have EAs smaller than the photon energy and thus are depleted by the laser. For ion beams with a strong, non-photodetachable background component at the same mass, no significant change in ion residence time is expected to occur. As background currents of several hundred nA at the mass of the trace ion species of interest are rare, this however is not expected to limit the applicability of this method for AMS-measurements. The high currents of several hundred nA for this study were only motivated by the necessity of current measurements of the transmitted filtered ion beam with Faraday cups as no suitable means of single particle counting in the presence of laser light is available at the ILIAS test bench. Further experiments in the saturation behavior are needed to pin down the individual contributions of the above described processes.

Optical filtering application

In order to validate the elemental selectivity of this technique, the composition of an ion beam extracted from a mixed target material was analyzed both before the ion cooler as well as after undergoing selective optical filtering. The sputter target for this study was a mix of Al_2O_3, MgO and ^{35}Cl enriched AgCl pressed into a copper cathode. The composition of the ion beam was analyzed by scanning the magnetic field of the analyzing magnet versus the current in the respective Faraday cups (cf. Figure 5). The whole system was initially tuned for both $^{35}Cl^-$ and AlO^-. All components of the cooler and the injector other than the analyzing magnet were then set to intermediate values and kept constant during the experiment. As a consequence, the transmission through the ILIAS cooler was rather low at 10% both for mass 43 and 35 during that experiment, but can be expected to be at the same level or even slightly higher for masses in between.

First the ion beam was mass-analyzed via current-detection in the cup in front of the ILIAS cooler. The same magnetic field range was then scanned versus the ion current behind the cooler with 0.20 mbar of He buffer gas. Finally, the laser was turned on and the composition of the ion beam analyzed in the same way. Each mass scan took approximately 5 min with about 1 min in between individual scans. Since the target had been sputtered for more than 2 hours prior to the actual experiment, it is very unlikely that the composition of the ion beam extracted from the source changed significantly during the total measurement time of roughly 20 min. This was also confirmed by repeated measurements of the $^{35}Cl^-$ and AlO^- currents in front of the ion cooler following the experiment.

The results of this study are plotted in Figure 8. The mass spectrum of the ion beam extracted from the ion source exhibits peaks from Cl^-, AlO^-, O_2^-, S^- and MgO^- as well as several other molecular anions. When the 532 nm laser is turned on, the anticipated drastic change in the anion beam composition after the ion cooler is observed. In the presence of 10.8 W of laser light, only ions with EAs larger than 2.33 eV pass the ion cooler unaffected, most notably Cl^- and AlO^-. All ion species with EAs lower than the photon energy such as O_2^-, S^- and MgO^- are selectively depleted by several orders of magnitude to intensities below the detection limit of the Faraday cup of around 1 pA. For MgO^-, e.g., an isobaric suppression factor of at least 10^4 against AlO^- is observed. The exact degree of selective ion beam purification remains to be determined with better means of ion identification.

As can be seen in Figure 8, buffer gas cooling of the anion beam alone also slightly influences the elemental composition due to selective depletion of weakly bound ion species caused by collisional detachment. The injection energy of 50 eV for this experiment was chosen for best transmission of Cl^- and AlO^-. Nevertheless, a strong depletion of MgO^- was also observed at

much lower injection energies, where collisional detachment was expected to be negligible based on kinematics and EA. Whether this points to an effective collisional detachment threshold with He well below the EA, as reported e.g. for O_2^- [29], or some other reason that accounts for this behavior remains to be investigated.

4. Conclusions and outlook

As part of the commissioning of the ILIAS ion beam cooler, atomic and molecular ion beams with intensities of several hundred nA were retarded long enough to allow continuous element-selective laser depletion of unwanted ion species by at least 5 orders of magnitude. Losses for the ion species of interest at the same time were below 50% and caused by the limited phase space acceptance of the system and collisional losses during cooling. This compares well to existing isobar suppression techniques at AMS-facilities such as degrader foils or gas filled magnets, where often much higher total beam losses have to be accepted to reduce isobaric interferences to manageable levels [31, 32]. Since the degree of suppression is not mass dependent, this technique clearly has the potential to broaden the spectrum of trace isotopes accessible with AMS in the mass region above 100 amu.

In several cases such as Co^-, MgO^- and S^-, the actual degree of suppression could in fact be much higher than observed here; the measurement sensitivity at the test bench was limited by the available means of ion beam monitoring and the lack of unambiguous ion identification techniques to analyze the optically filtered ion beam at the test bench. These issues will be resolved in the near future by coupling the ILIAS cooler to the VERA AMS-facility. For this purpose, the VERA injector has already been extended to accommodate the ILIAS cooler. Currently, the photodetachment setup is reassembled at VERA and first experiments are expected to take place within the next months. Future experiments will also benefit from the new resonant RF setup providing stronger transversal ion confinement and thus will help reduce beam losses caused by space charge.

Apart from the endeavor for new AMS trace isotopes, one of the first isotopes to profit from this novel technique is likely to be ^{26}Al. While most AMS measurements of ^{26}Al suffer from the low probability of Al^- formation, use of the much more prolific AlO^- ion is hindered by the strong interference of MgO^- and thus was limited to a few facilities with ample terminal voltage [33, 34]. The optical filtering method can provide selective suppression of MgO by at least four orders of magnitude. This may allow even medium-sized facilities like VERA to use AlO^- for injection and thereby boost the overall ^{26}Al detection efficiency by more than a factor of 5.

Acknowledgments

The authors express their gratitude to Prof. Dr. Clemens Walther, University of Hannover, for providing the 400W RF-amplifier. This work was supported by the Austrian Science Fund (FWF) (grant P 22164-N20) and by the University of Vienna (Investitionsprojekte 2011, 2012, 2013, 2015). DH and PA acknowledge support from the Swedish Research Council.

References:

[1] R.C. Finkel and M. Suter, Advances in Analytical Geochemistry 1 (1993) 1.

[2] W. Kutschera, International Journal of Mass Spectrometry 242 (2005) 145.

[3] A.E. Litherland, I. Tomski, X.-L. Zhao, L.M. Cousins, J.P. Doupe, G. Javahery and W.E. Kieser, Nucl. Instr. and Meth. B 259 (2007) 230.

[4] D. Berkovits, E. Boaretto, G. Hollos, W. Kutschera, R. Naaman, M. Paul and Z. Vager, Nucl. Instr. and Meth. A 281 (1989) 663.

[5] H.A. Synal, International Journal of Mass Spectrometry 349-350 (2013) 192.

[6] M. Martschini, J. Buchriegler, P. Collon, W. Kutschera, J. Lachner, W. Lu, A. Priller, P. Steier and R. Golser, Nucl. Instr. and Meth. B 361 (2015) 201.

[7] J. Lachner, M. Kasberger, M. Martschini, A. Priller, P. Steier and R. Golser, Nucl. Instr. and Meth. B 361 (2015) 440.

[8] O. Forstner, H. Gnaser, R. Golser, D. Hanstorp, M. Martschini, A. Priller, J. Rohlen, P. Steier, C. Vockenhuber and A. Wallner, Nucl. Instr. and Meth. B 269 (2011) 3180.

[9] W.E. Kieser, X.-L. Zhao, A.E. Litherland, J. Eliades and R.J. Cornett, EPJ Web of Conferences 63, (2013) 03005.

[10] J. Eliades, A.E. Litherland, W.E. Kieser, L. Cousins, S.J. Ye and X.-L. Zhao, Nucl. Instr. and Meth. B 268 (7-8) (2010) 839.

[11] Y. Liu, J.R. Beene, C.C. Havener and J.F. Liang, Appl. Phys. Lett. 87 (2005) 113504.

[12] P. Andersson, A.O. Lindahl, D. Hanstorp, C.C. Havener, Yun Liu and Yuan Liu, J. Appl. Phys. 107 (2010) 026102.

[13] O. Forstner, P. Andersson, D. Hanstorp, J. Lahner, M. Martschini, J. Pitters, A. Priller, P. Steier and R. Golser, Nucl. Instr. and Meth. B 361 (2015) 217.

[14] J.C. Rienstra-Kiracofe, G.S. Tschumper, H.F. Schaefer, S. Nandi and G.B. Ellison, Chemical Reviews 102 (2002) 231.

[15] T. Andersen, H. Haugen and H. Hotop, Journal of Physical and Chemical Reference Data 28 (6) (1999) 1511.

[16] F. Herfurth, J. Dilling, A. Kellerbauer, G. Bollen, S. Henry, H.-J. Kluge, E. Lamour, D. Lunney, R. Moore, C. Scheidenberger, S. Schwarz, G. Sikler and J. Szerypo, Nucl. Instr. and Meth. A 469 (2) (2001) 254.

[17] Y. Liu, J. Liang, G. Alton, J. Beene, Z. Zhou and H. Wollnik, Nucl. Instr. and Meth. B 187 (1) (2002) 117.

[18] A. Nieminen, J. Huikari, A. Jokinen, J. Äystö, P. Campbell and E. Cochrane, Nucl. Instr. and Meth. A 469 (2) (2001) 244.

[19] A. Kellerbauer, T. Kim, R. Moore, and P. Varfalvy, Nucl. Instr. and Meth. A 469 (2) (2001) 276.

[20] J. Pitters, *Laser Photodetachment in a Gas-Filled RF-Quadrupole*, master thesis at the University of Vienna (2015).

[21] D. R. Denison, Journal of Vacuum Science and Technology 8 (2) (1971) 266.

[22] F. Major, V. Gheorghe and G. Werth, Charged Particle Traps. Heidelberg: Springer, 2006.

[23] T. Moreau, *Development and characterization of the Ion Laser InterAction Setup (ILIAS)*, master thesis at the University of Vienna (2016)

[24] Y. Liu, J.F. Liang and J.R. Beene, Nucl. Instr. and Meth. B 255 (2007) 416.

[25] R. Boussaid, G. Ban and J.F. Cam, Phys. Rev. ST Accel. Beams 18 (2015) 072802.

[26] M.S. Huq, L.D. Doverspike, R.L. Champion and V.A. Esaulov, J. Phys. B: At. Mol. Phys. 15 (1982) 951.

[27] F. Penent, J.P. Grouard. R.I. Hall, J.L. Montmagnon, R.L. Champion, L.D. Doverspike and V.A. Esaulov, J. Phys. B: At. Mol. Phys. 20 (1987) 6065.

[28] R.L. Champion, Advances in Electronics and Electron Physics 58 (1982) 143.

[29] M.J. Wynn, J.D. Martin and T.L. Bailey, The Journal of Chemical Physics 52 (1970) 191.

[30] http://simion.com/info/surface_enhancement.html

[31] R. Finkel, M. Arnold, G. Aumaitre, L. Benedetti, D. Bourles, K. Keddadouche and S. Merchel, Nucl. Instr. and Meth. B 294 (2013) 121.

[32] V. Alfimov, G. Possnert and A. Aldahan, Nucl. Instr. and Meth. B 259 (2007) 199.

[33] A. Arazi, T. Faestermann, J.O. Fernandez Niello, D. Frischke, K. Knie, G. Korschinek, H.J. Maier, E. Richter, G. Rugel and A. Wallner, Nucl. Instr. and Meth. B 223-224 (2004) 259.

[34] L.K. Fifield, S.G. Tims, L.G. Gladkis and C.R. Morton, Nucl. Instr. and Meth. B 259 (2007) 178.

Figure captions

Figure 1: (a) Schematic drawing of the ILIAS RFQ ion cooler including experimental pressure values in various sections during operation with He buffer gas. Electric insulators are drawn in grey. The red colors in the online version indicate different electric potentials for the respective parts. (b) Photo of the ILIAS RFQ ion cooler showing the electrode structure with the entrance aperture dismounted. The electrode structure consists of four RF-rods and four guiding electrodes held by spacers made of Macor. (c) Photo of the same cooler end with the insulated entrance aperture mounted. The size of the pumping holes in the tube wall can be adjusted with the sliding sleeves.

Figure 2: Transmitted ion current plotted in black (online blue) and ion current on the extraction aperture plotted in grey (online red) as a function of He buffer gas pressure. With increasing buffer gas pressure, also ions with initially large radii from the cooler axis are migrating towards the center, such that they are transmitted through the exit aperture rather than lost on it. This is a clear indication of successful ion beam cooling. The data was recorded with 300 nA of AlO^- injected into the cooler, 160 V zero to peak RF voltage and an RF frequency of 2.1 MHz.

Figure 3: Ion beam transmission through the ILIAS cooler. (a) Normalized transmitted currents as a function of the Mathieu parameter q for three different anion species. The data was recorded at a He buffer gas pressure of 0.20 mbar and a zero-to-peak RF voltage of 100 V at varying RF frequencies. Injected currents were 25 nA for $^{35}Cl^-$, 150 nA for AlO^- and 360 nA for $^{63}Cu^-$. Highest transmission values are achieved at q between 0.4 and 0.5. (b) Transmission as a function of injected current for a $^{63}Cu^-$ beam. The data was recorded at 0.16 mbar He pressure, 200 V zero-to-peak RF voltage and an RF frequency of 2.0 MHz. No prior beam collimation was done and the transmission calculated as the ratio between injected and extracted ion current. The obvious decrease in transmission at currents of several hundred nA is due to space charge effects.

Figure 4: Ion residence time distributions for a $^{63}Cu^-$ beam under different operating conditions of the ILIAS cooler derived from the current pulse characteristics of a chopped ion beam. The plotted times also include around 40 μs time of flight outside the ion cooler. (a) Residence time distributions for 3.2 nA of injected ion current at 0.30 mbar of buffer gas pressure under different operating conditions. The strength of the longitudinal guiding field has only a minor influence on the residence times. The strong offset when studying the rising edge of a current pulse may be linked to the build-up of space charge. (b) Residence time distributions at various

buffer gas pressures for 3.2 nA of injected ion current. (c) Residence time distributions for various injected ion currents at a buffer gas pressure of 0.30 mbar. Note the logarithmic time scale and significant variation of residence times with current.

Figure 5: Schematic drawing of the experimental setup for the photodetachment experiments at ILIAS. The mass-separated ion beam is injected into the ion cooler and collinearly overlapped with the laser beam. Transmitted anions are reaccelerated and bent out of the laser beam for detection by an electrostatic quadrupole beam bender. Components for the TOF-measurements described in section 3.1 are also shown.

Figure 6: Transmitted ion current plotted in grey (online blue) as a function of time while the laser was turned on and off periodically in intervals of typically 15 seconds each. The transmitted laser power is plotted in black (online green). The power overshoot at the beginning of each laser pulse is an artifact from the calorimetric power head. The data was recorded at 0.25 mbar He pressure. (a) $^{63}Cu^-$ with an EA of 1.23578(4) eV is depleted via photodetachment by more than 5 orders of magnitude with the 532 nm laser corresponding to 2.33 eV photon energy. (b) $^{127}I^-$ with an EA of 3.059038(10) eV remains unaffected by the laser with 2.33 eV photon energy under the very same conditions.

Figure 7: Photodetachment suppression factors for $^{63}Cu^-$ as a function of laser power for three different He buffer gas pressures. The power of the 532 nm laser was adjusted by rotation of the polarization plane and subsequent beam splitting to maintain constant power profiles. Where not shown, error bars are smaller than the plotted symbols.

Figure 8: Comparison of mass spectra of an ion beam extracted from a mixed target material (Al_2O_3 + MgO + ^{35}Cl enriched AgCl) before and after undergoing cooling and selective optical filtering in the ion cooler. Experiments were performed at 0.20 mbar He pressure and 10.8 W of transmitted 532 nm laser power. The electron affinities of prolific ion species are given in parentheses in units of eV. Only ion species with electron affinities below the photon energy of 2.33 eV are depleted via laser photodetachment. The reason for the substantial suppression of MgO^- by buffer gas cooling alone is still under investigation.

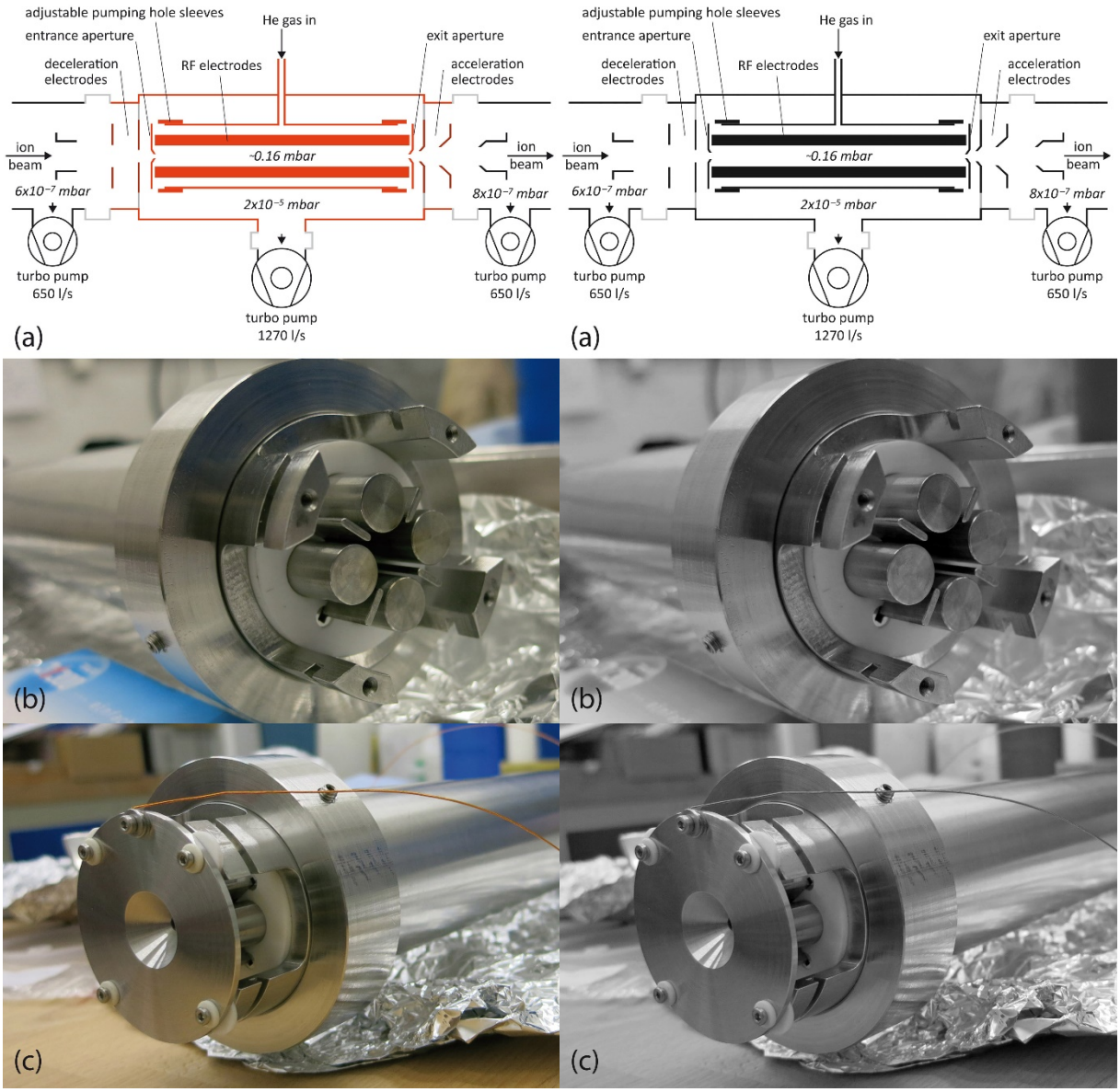

Figure 1 and Figure 1_bw

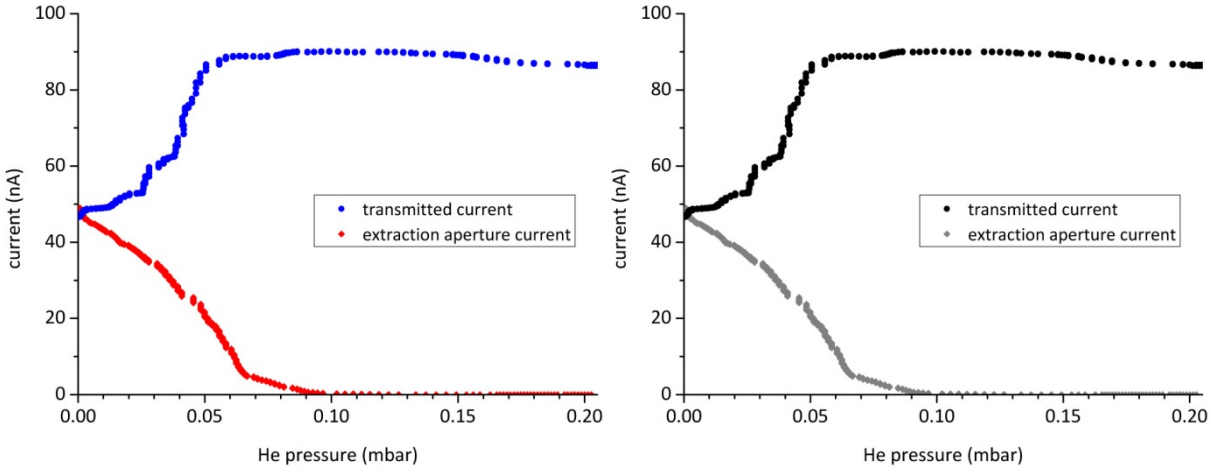

Figure 2 and Figure 2_bw

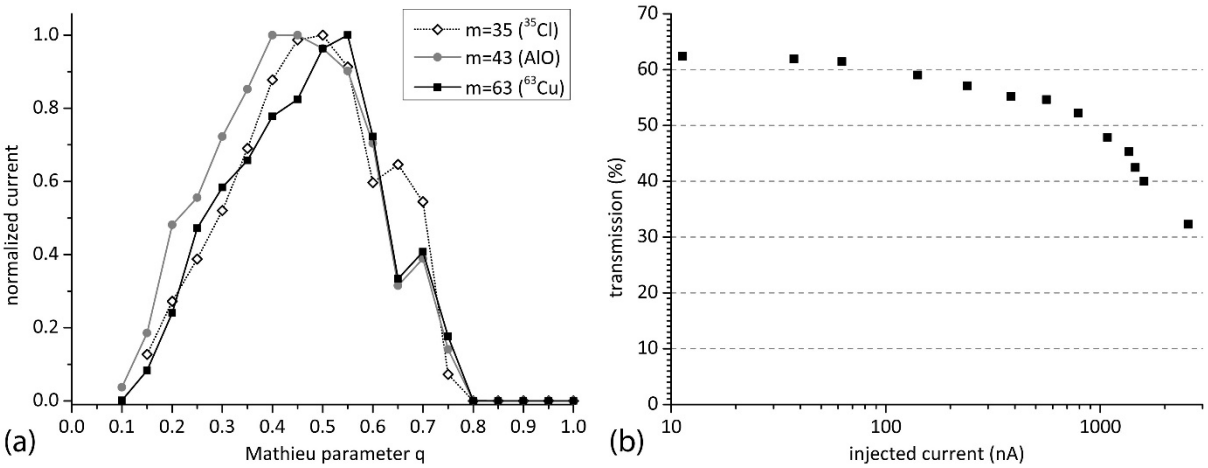
m=35 (^{35}Cl)
m=43 (AlO)
m=63 (^{63}Cu)
normalized current
Mathieu parameter q
(a)
transmission (%)
injected current (nA)
(b)

Figure 3

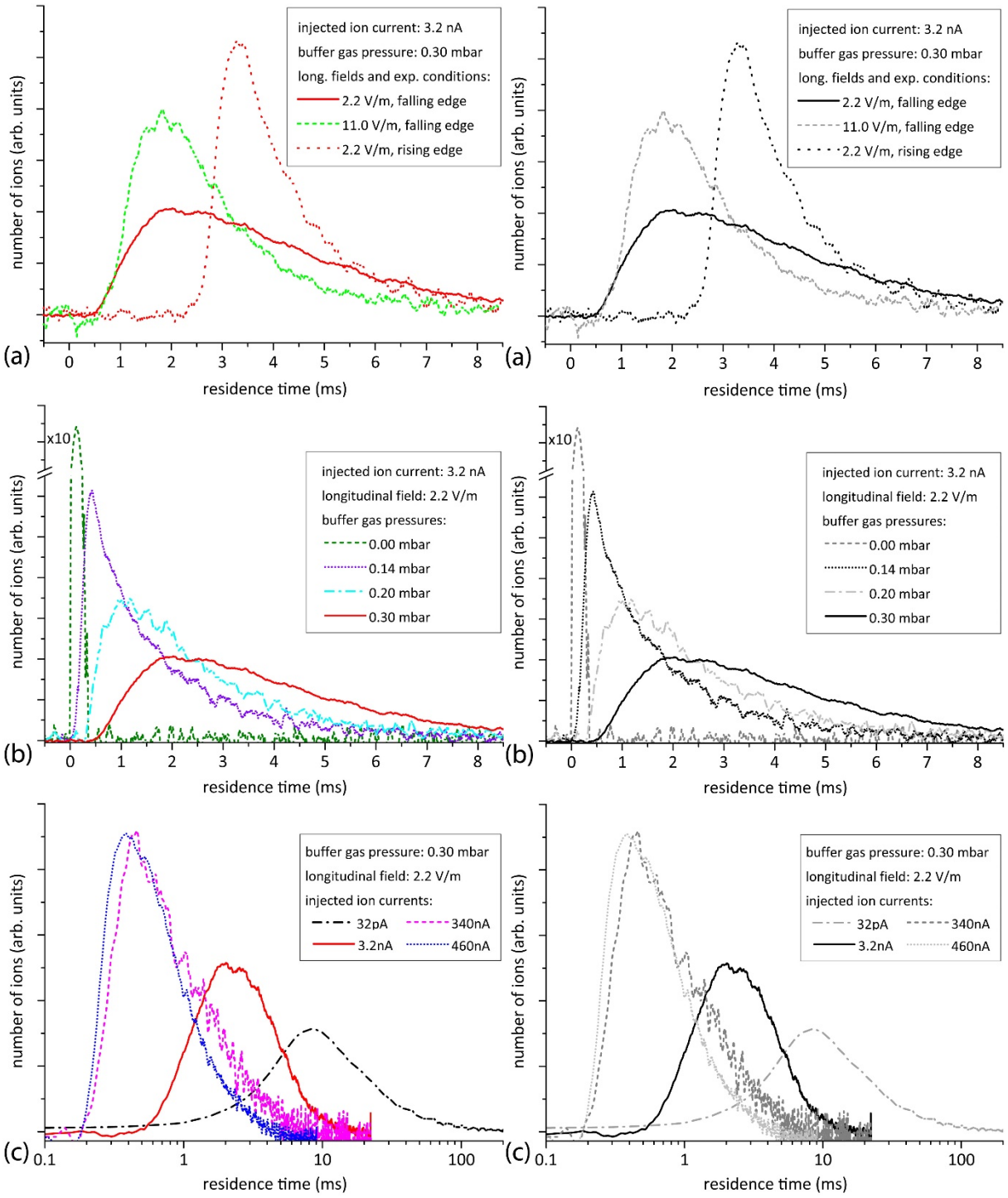

Figure 4 and Figure 4_bw

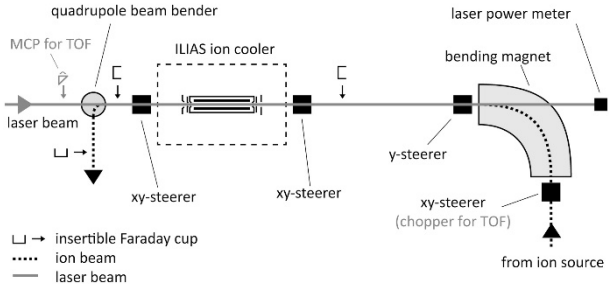
quadrupole beam bender
MCP for TOF
ILIAS ion cooler
laser power meter
bending magnet
laser beam
y-steerer
xy-steerer
xy-steerer
xy-steerer
(chopper for TOF)
from ion source
insertible Faraday cup
ion beam
laser beam

Figure 5

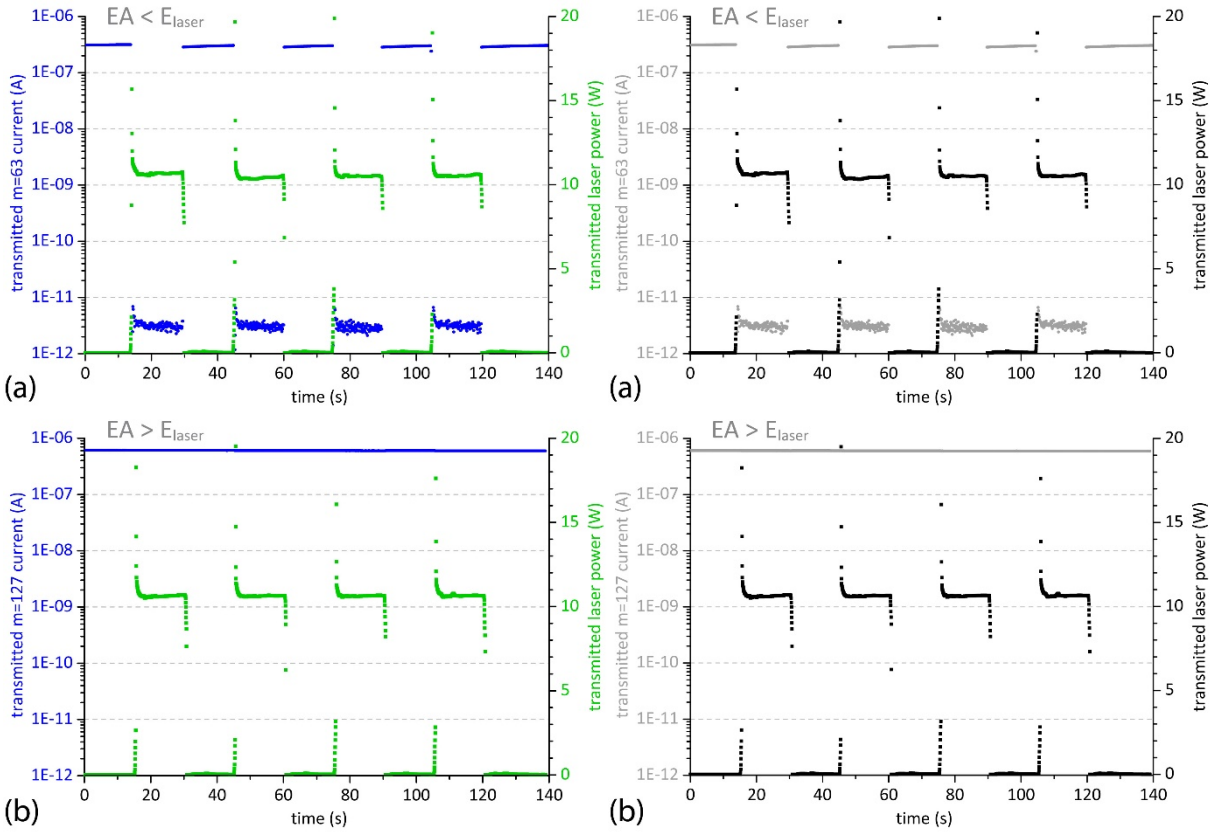

Figure 6 and Figure 6_bw

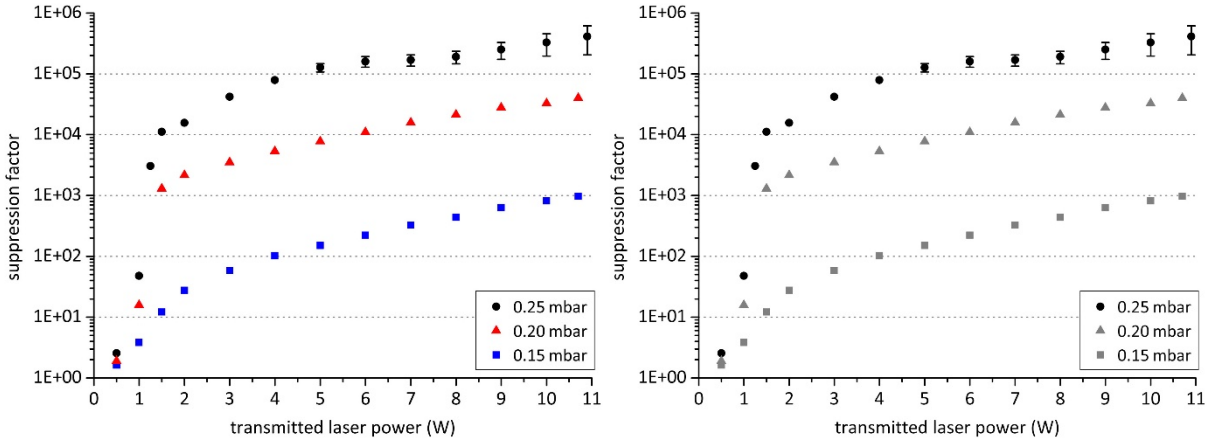

Figure 7 and Figure 7_bw

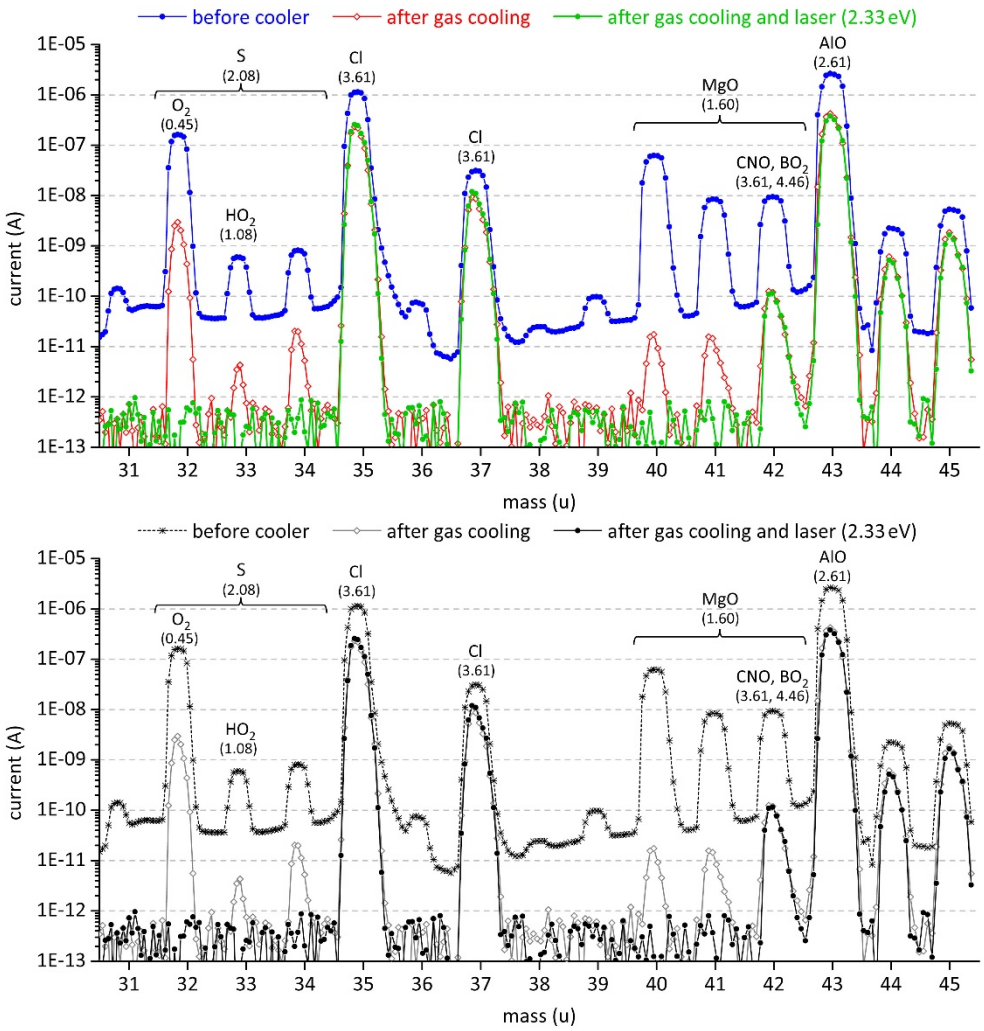

Figure 8 and Figure 8_bw

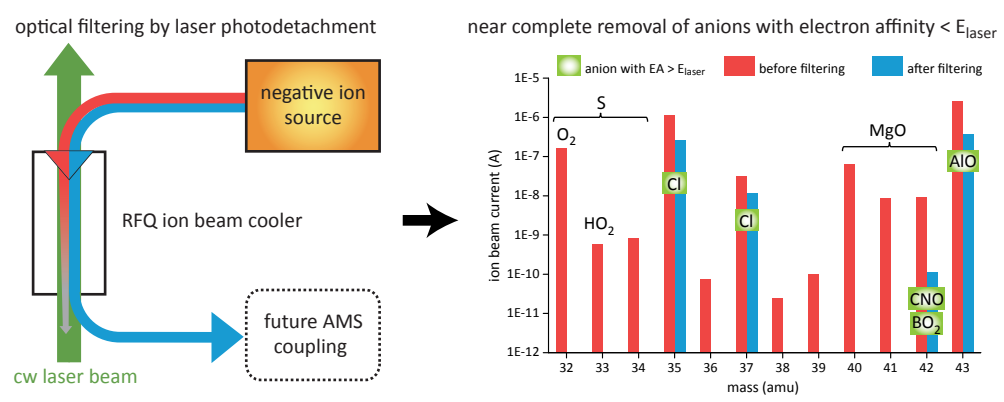
optical filtering by laser photodetachment
negative ion source
RFQ ion beam cooler
future AMS coupling
cw laser beam
near complete removal of anions with electron affinity < E_laser
anion with EA > E_laser
before filtering
after filtering
ion beam current (A)
mass (amu)
S
O2
HO2
Cl
Cl
MgO
AlO
CNO
BO2